The effects of flank collapses on volcano plumbing systems

Andrea Manconi[1]*, Marc-Antoine Longpré[2,3], Thomas R. Walter[1], Valentin R. Troll[2,4], and Thor H. Hansteen[5]

[1]GFZ German Research Centre for Geoscience, Telegrafenberg, 14473 Potsdam, Germany
[2]Trinity College Dublin, College Green, Dublin 2, Ireland
[3]Earth and Planetary Sciences, McGill University, 3450 University St., Montréal, Québec H3A 2A7, Canada
[4]Uppsala University, 16 Villav., 752 36 Uppsala, Sweden
[5]IFM-GEOMAR, Wischhofstrasse 1-3, D-24148 Kiel, Germany

ABSTRACT

The growth of large volcanoes is commonly interrupted by episodes of flank collapse that may be accompanied by catastrophic debris avalanches, explosive eruptions, and tsunamis. El Hierro, the youngest island of the Canary Archipelago, has been repeatedly affected by such mass-wasting events in the last 1 Ma. Our field observations and petrological data suggest that the largest and most recent of these flank collapses—the El Golfo landslide—likely influenced the magma plumbing system of the island, leading to the eruption of higher proportions of denser and less evolved magmas. The results of our numerical simulations indicate that the El Golfo landslide generated pressure changes exceeding 1 MPa down to upper-mantle depths, with local amplification in the surroundings and within the modeled magma plumbing system. Stress perturbations of that order might drastically alter feeding system processes, such as degassing, transport, differentiation, and mixing of magma batches.

INTRODUCTION

Catastrophic, large-scale flank collapses punctuate the evolution of many volcanic edifices. Modern volcanology took a quantum leap in the aftermath of 18 May 1980, as Mount St. Helens (Washington, United States) was the site of the largest flank collapse and one of the most spectacular volcanic eruptions in recorded history. Since then, evidence of such flank collapse, in the form of amphitheater-like reentrants carved into volcanic edifices or remnants of related slump and debris avalanche deposits, has been identified at numerous stratovolcanoes (e.g., McGuire, 1996). Oceanic shield volcanoes too are subject to flank collapse during their lifetime. While lateral collapses on continental stratovolcanoes generally have volumes of 10^3–10^5 m^3 and worldwide repeat intervals of 10^2–10^3 a, giant slumps on oceanic islands involve volumes as large as 10^9–10^{12} m^3 and recur every 10^4–10^6 a (McGuire, 1996). Due to their enormous destructive potential, volcano flank collapses and associated hazards require a sustained level of research on their causes and effects (McGuire, 1996, and references therein).

The collapse of a volcano flank probably has permanent effects on the edifice's morphology as well as on the local volcano-tectonic regime (e.g., Lipman et al., 1991). Recent studies indicate that flank collapse events at both stratovolcanoes and oceanic shield volcanoes may be followed by rapid constructional phases and changes in erupted lava compositions (e.g., Hildenbrand et al., 2004; Hora et al., 2007). These apparent variations in the volcanic and magmatic regimes are thought to be due to the static decompression at depth after surface unloading and its potential influence on magma chamber processes (Pinel and Jaupart, 2005), and perhaps even on mantle melt production (Presley et al., 1997). This is by analogy similar to the effect of ice unloading during deglaciation periods in Iceland, which has been shown to drastically affect local volcanism (e.g., Sigvaldason et al., 1992; Jull and McKenzie, 1996). However, no quantitative models have yet tested the postulated relationships between volcano flank collapse and subsequent volcanism.

Our field observations and the analysis of volcanic products summarized herein suggest that a large and recent flank collapse, the El Golfo landslide, likely affected the magmatic regime of El Hierro Island, in the Canary Archipelago. We present finite-element models that simulate the unloading of realistic fractions of a volcanic edifice, using El Hierro as an exemplary case. The modeling results show that the decompression generated by volcano flank collapse is able to induce pressure gradients and instability in a magma storage zone and its surroundings, probably accounting for drastic effects on magma plumbing and eruptive dynamics.

BACKGROUND

El Hierro is the youngest, smallest, and westernmost of the Canary Islands (Fig. 1), and it is currently in its "shield-stage period" (Carracedo et al., 2001). The island is formed by a group of coalescent volcanoes, which all show evidence of mass-wasting events. The oldest, now concealed Tiñor collapse (age 882–545 ka) preceded the El Julán landslide (~130 km^3, age ~200 ka), which affected the southwest side of the island. In addition, two of the most recent large-scale flank collapses on Atlantic volcanoes occurred on El Hierro. The Las Playas debris avalanche (25–50 km^3, age between 176 and 145 ka) formed a prominent coastal embayment on the southeast flank of the island. Most recently, however,

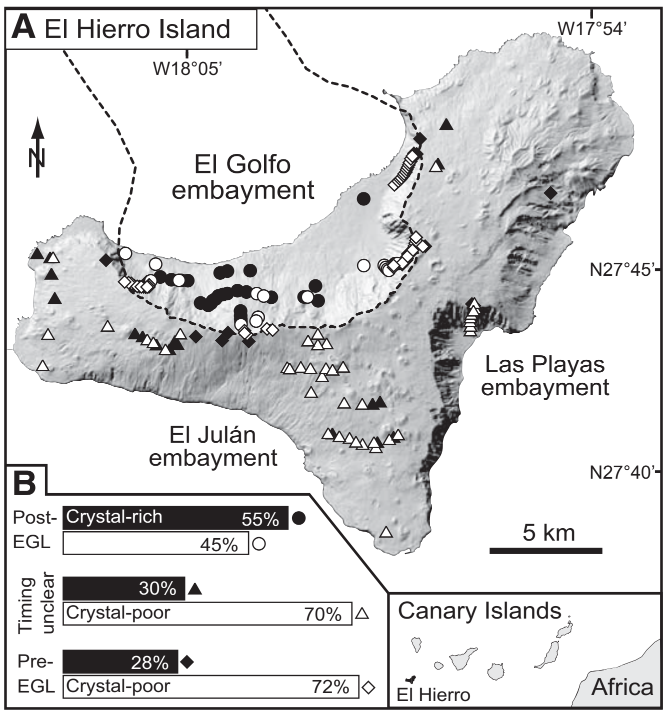

Figure 1. Shaded relief map of El Hierro Island. (A) Dashed lines show extent of El Golfo landslide (EGL) scar and deposits. Symbols represent sampling and/or investigated outcrop localities. (B) Histogram showing that ankaramitic, "crystal-rich" volcanics (black bars) have out-proportioned eruptions compared to all other lava types (white bars) in recent, post-EGL volcanic phase of El Hierro.

*Current address: IREA-CNR (Istituto per il Rilevamento Elettromagnetico dell' Ambiente–Consiglio Nazionale delle Ricerche), Via Diocieziano 328, 80124 Naples, Italy.

the El Golfo landslide removed an enormous portion (150–180 km^3; Masson et al., 2002) of El Hierro's northwest flank, producing a vast and well-preserved scar—the El Golfo embayment. Published K-Ar dates imply that this catastrophic debris avalanche is younger than 134 ka but older than 21 ka (Carracedo et al., 2001).

The magma plumbing system feeding volcanism at El Hierro was recently investigated using clinopyroxene-melt thermobarometry (Stroncik et al., 2009). Phenocrysts retrieved from submarine lava flows yield crystallization depths in the range of 19–26 km below sea level, suggesting that magmas are stored in a multilevel plexus of dike- and sill-like fractures in the uppermost mantle. Moreover, the crystals' complex zoning patterns indicate that mixing of moderately evolved and mafic magmas is an important process beneath El Hierro, as for other Canary Island volcanoes (e.g., Klügel et al., 2005; Stroncik et al., 2009).

Field and Petrological Evidence

We conducted detailed field campaigns on El Hierro to determine whether the El Golfo landslide may have had observable effects on subsequent volcanism. Mapping of lava-type distribution, logging of well-exposed stratigraphic sections, and sampling were carried out at strategic localities, particularly in the vicinity of the El Golfo embayment. Our field and petrological analysis indicates that, from ca. 261 to 176 ka, the volcano emitted differentiated products, including lavas and block and ash flows of trachytic composition (up to 60 wt% SiO_2 and 0.9 wt% MgO), consistent with findings by Carracedo et al. (2001). Such evolved units are absent from the sequence of lava flows that have started to fill the El Golfo embayment (which are thus younger than 134 ka). Indeed, these postlandslide eruptions have involved significantly more mafic basanitic magmas (mean of 44 wt% SiO_2 and 8.5 wt% MgO) that are often charged with abundant and large olivine and clinopyroxene crystals. Eruptions of these crystal-rich lavas (>20 vol% clinopyroxene + olivine, hereafter referred to as ankaramites) appear to have outnumbered eruptions of other lava types in the recent postlandslide eruptive phase (Fig. 1B). Magma density calculations indicate that ankaramites are substantially denser than other El Hierro magma types, with $\rho = 2950 \pm 50$ kg/m^3 compared with 2810 ± 80 kg/m^3 for moderately phyric basalts, 2660 ± 60 kg/m^3 for aphyric basalts, and 2390 ± 40 kg/m^3 for trachytes. For more details about the field and the petrological data, see the GSA Data Repository.[1]

These results suggest that the recent flank collapses—most particularly the El Golfo landslide—have considerably disturbed the island's magmatic regime, apparently causing higher proportions of substantially denser and less evolved magmas to erupt.

FINITE-ELEMENT MODELS

To verify whether the perturbations of El Hierro's volcanic regime might indeed be related to the effects of large-scale mass wasting, we constructed finite-element models using the El Golfo landslide as a collapse-type example (Fig. 2A). We modeled El Hierro Island as a conical edifice loading the oceanic lithosphere, which is represented as an elastic half-space. We then removed 3% of the island's initial weight, simulating a rapid unloading equivalent to the El Golfo landslide volume estimates (Masson et al., 2002). Variations of mean stress at depth are defined as:

$$\Delta P = -\frac{1}{3}\sigma_{kk}, \quad (1)$$

where σ_{kk} is the trace of the stress tensor, and ΔP is hereafter referred to as decompression.

The simulations were first performed assuming homogeneous material throughout. Secondly, we introduced a mechanically softer region that is oblate in shape (semi-axes ratio 2/5 km) and centered at a depth of 20 km below the seafloor, aiming to model the upper-mantle magmatic system of El Hierro (Stroncik et al., 2009). The elastic properties of this "zone" were assumed to be dependent on the percentage of melt present within it (see the Data Repository).

MODELING RESULTS

In the model, the surface unloading caused by the El Golfo landslide induces decompression of the lithosphere at amplitudes that decay exponentially with depth (Fig. 2B). The pressure drop of ~4 MPa directly beneath the El Hierro edifice decreases to ~0.5–0.6 MPa at the main magma storage levels (18–22 km depth). Heterogeneous models show that large pressure gradients develop in the surroundings of, as

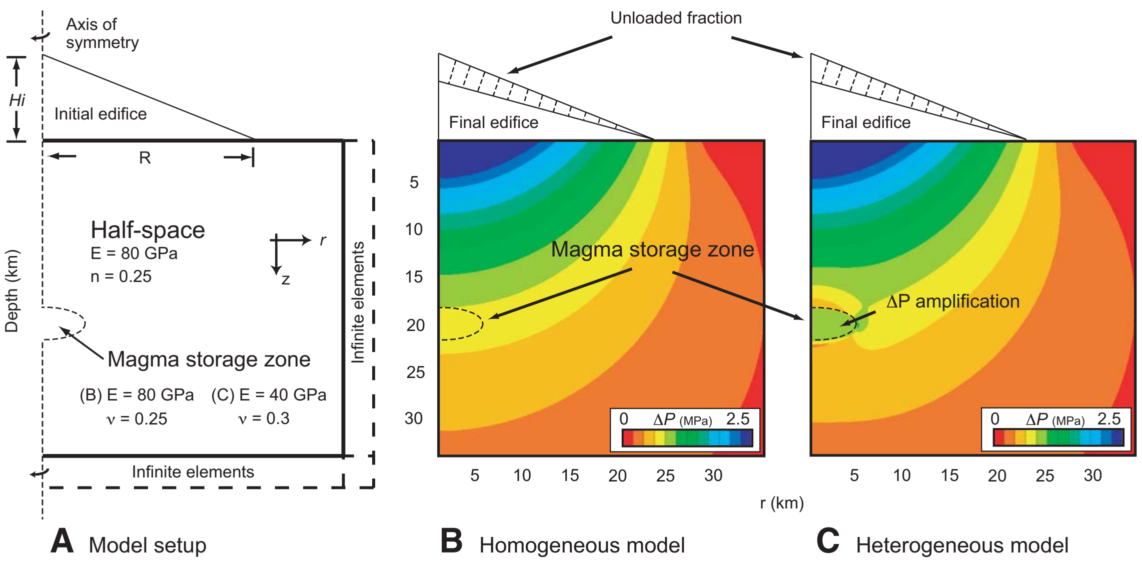

Figure 2. Finite-element models (FEM) of El Golfo landslide unloading El Hierro edifice. (A) FEM setup.Initial edifice rises above seafloor (height [*Hi*] = 6 km, radius [R] = 30 km). Far-field boundary conditions are simulated by imposing a set of infinite elements at bottom and on right side of model. Resolution of elements in near field is 100 m. Elastic properties of half-space are defined by Young's modulus (E) and Poisson's ratio (ν). (B–C) Pressure changes after unloading within homogeneous and heterogeneous models, respectively. In C, local stress gradients are observed inside and in surroundings of a mechanically softer zone (dashed line) that simulates magma storage region.

[1]GSA Data Repository item 2009272, details on the densities of El Hierro volcanic products and the finite element modeling assumptions and limitations, and additional dicussion of the results, is available online at www.geosociety.org/pubs/ft2009.htm, or on request from editing@geosociety.org or Documents Secretary, GSA, P.O. Box 9140, Boulder, CO 80301, USA.

well as within, the softer magma reservoir (Fig. 2C). Decompression in this zone differs by up to 50% from that obtained within a homogeneous half-space.

Within the modeled magma plumbing system, volumetric expansion occurs and reaches up to 30 μ strain. Larger values in the upper levels of the magma storage zone compared to its lower parts lead to pressure gradients of ~0.1 MPa (Figs. 3A and 3B). Viscous effects of the upper mantle, not considered in our models, may amplify these values on a longer time scale. The pattern and the amplitude of such differential pressure are not significantly affected when different depths, mechanical contrasts, and/or various shapes of the magma reservoir are considered (see the Data Repository).

Our models thus suggest that the El Golfo landslide induced pressure changes and gradients at depth within El Hierro's magma reservoirs, providing likely candidates for sudden disturbances of magma plumbing dynamics.

SUMMARY AND DISCUSSION

Recent studies have shown that static and/or dynamic volumetric expansion associated with earthquakes can trigger volcanic unrest. Volatile exolution, bubble nucleation, and mingling and mixing of different magma batches are encouraged, thus increasing the probability of eruption (Manga and Brodsky, 2006). According to our models, the El Golfo landslide would have caused volumetric expansion up to five times larger than that inferred for Córdon Caulle, a volcano in the Central Andes, where an eruption was triggered after the 1960 M_w 9.5 megathrust earthquake in Chile (Walter and Amelung, 2007).

Moreover, we have shown that mechanical contrast between the magma storage region and the surrounding rock is a key parameter controlling the amplitudes of landslide-induced decompression. Indeed, variations of tensile stresses in the mechanically softer storage zone, especially at its lateral peripheries, reach up to 2.5 MPa after the simulated flank collapse. Stress variations of such amplitudes, also due to mass unloading, have been shown to promote fracture initiation and eventual magma propagation (Andrew and Gudmundsson, 2007). In this context, El Hierro's latest flank collapse and the associated stress changes at depth appear more than sufficient to have caused perturbations in eruptive activity.

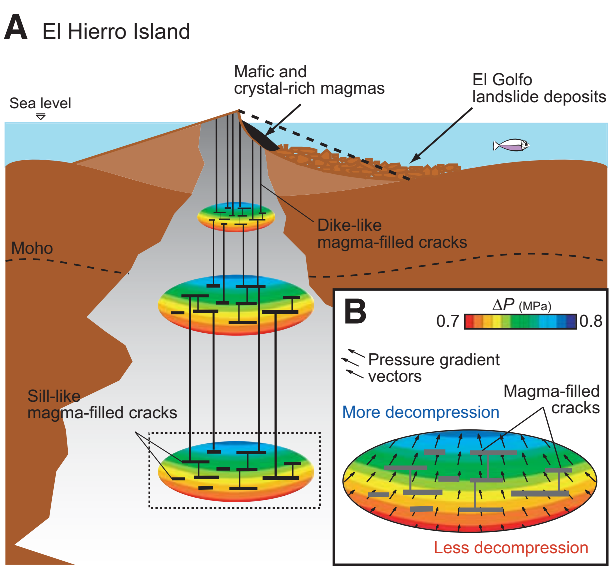

Figure 3. Sketch of El Golfo landslide and its potential effects on El Hierro's magma plumbing system. (A) Broad magma storage regions beneath El Hierro are represented as oblate-shaped reservoirs. Black solid lines represent sill- and dike-like magma-filled fractures (cf. Stroncik et al., 2009). (B) Details of a magma storage zone located at ~20 km below seafloor (dashed rectangle in A). Decompression induces magma degassing and pressure gradients that favor remobilization, ascent, and mixing of different magma batches (black arrows).

Comparison to Other Volcanic Systems

Evidence of landslide-related perturbations in the magmatic and eruptive regimes has been reported from both stratovolcanoes and intraplate basaltic shield volcanoes. At Mount St. Helens, for example, past lateral collapses are thought to have provoked a return to more mafic magma compositions (Pinel and Jaupart, 2000). Similarly, erupted magmas at Bezymianny volcano, Kamchatka, Russia, are gradually becoming more mafic since its catastrophic sector collapse in 1956 (Izbekov et al., 2006). Parinacota volcano, northern Chile, has seen increased magma recharge rates, lesser degrees of fractionation, as well as a shift of the magma chamber to shallower levels after a late Pleistocene sector collapse (Ginibre and Wörner, 2007).

Regarding ocean-island volcanoes, Lipman et al. (1991) suggested that the lateral collapse associated with the formation of the southwest Hawaii slide complex on Mauna Loa volcano might have resulted in sudden, large phreatomagmatic eruptions from the landslide headwall. Presley et al. (1997) showed that Waianae volcano, on Oahu, erupted less differentiated magmas after a mass-wasting event some 6100 km^3 in volume. These authors proposed that, in addition to disturbing magma plumbing, the huge Waianae slump might have affected magma genesis in the mantle, in agreement with trace-element chemistry. Moreover, Hildenbrand et al. (2004) claimed that eruptive rates immediately after a collapse episode on the northern flank of Tahiti-Nui Island, French Polynesia, were 2–5 times higher than during the volcano's initial shield phase and later activity. Temporal changes in lava chemistry appear to correlate with this landslide and were interpreted as related to increased partial melting in the mantle due to collapse-induced decompression.

To test the general applicability of the El Hierro results, we applied our modeling approach to simulate the effects of lateral collapse at other volcanic edifices (Fig. 4). Overall, decompression amplitude depends on the volume of the collapsed sector; however, the ratio between the initial and the final load as well as the radius of the initial edifice control rapid or slow decay of the decompression effect. Therefore, mass-wasting events that occur at different volcano types and that have volumes differing by orders of magnitude may induce similar pressure changes at depth. For example, the flank collapses at the Teno massif, Tenerife, Canary Islands, would have caused pressure changes in the lithosphere similar to those calculated for the mass-wasting events at Parinacota volcano, Chile, and at Mount St. Helens in 1980 (50 km^3, 6 km^3, and 2.5 km^3, respectively; see the Data Repository).

However, despite available geochemical data in agreement with potential landslide-induced increases in melt fractions at Hawaii (Presley et al., 1997) and Tahiti-Nui (Hildenbrand et al., 2004), our modeling results imply very low decompression values at depths relevant to mantle melting, suggesting that an effect on melt production is unlikely (e.g., <<0.5 MPa at ~80 km depth beneath El Hierro; see also the Data Repository).

A Conceptual Model for Magma Remobilization after Flank Collapse

The load of a volcanic edifice acts as "a density filter" on the magmatic system (Pinel and Jaupart, 2000), i.e., the eruption of mafic, high-density magmas is hindered, and eruption of SiO_2-rich, low-density magmas is promoted, as a volcano grows in size. After flank collapse, however, the volcanic load above magma chambers and conduits is displaced and reduced, which should itself help to widen the density window of eruptible magmas. In addition, if magmas are volatile-oversaturated at depth, which is the case for mafic alkaline ocean-island magmas stored in the upper mantle (such as those of El Hierro; Hansteen et al., 1998; Stroncik et al., 2009), decompression is likely to enhance homogeneous bubble growth and nucleation. Gas expansion, and the

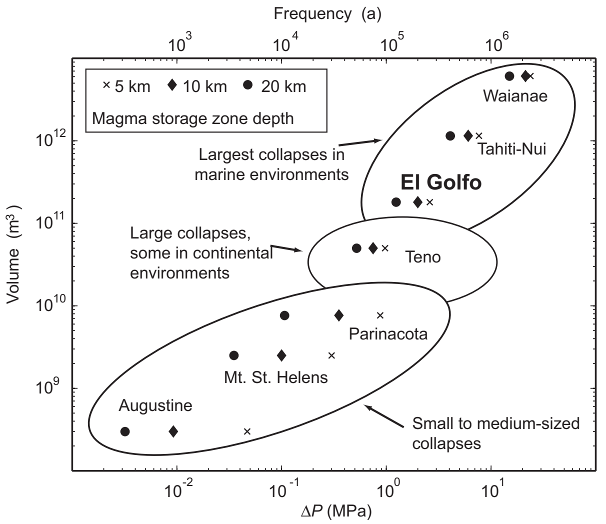

Figure 4. Landslide-induced decompression calculated for various volcanic systems. Log-scale axes show decompression (bottom *x*-axis), recurrence time (top *x*-axis, from McGuire, 1996) and flank-collapse volume (*y*-axis). Decompression is calculated assuming a mechanically softer reservoir at three different depths beneath edifices: 5 km (cross); 10 km (full diamond); 20 km (full circle). See text for details.

resulting increase in magma chamber pressure and effective decrease in magma density, ought to facilitate magma propagation and ascent, further increasing the probability of eruption of denser, more primitive, and crystal-rich magmas like ankaramites.

Furthermore, our modeling results show that a volcano flank collapse will induce relatively high-pressure gradients within magma reservoirs at depth (Figs. 3A and 3B). By comparison, an El Golfo–sized landslide produces differential pressures between the top and bottom of El Hierro's magmatic system that are on the same order of magnitude as those caused by large earthquakes, which have been shown to trigger subsurface fluid migration (Manga and Brodsky, 2006). Such fluid migration is thus also expected after flank collapse and will follow upward trajectories within the magma plumbing, as defined by the superimposed gradients (vectors in Fig. 3B). This process will bring fractional crystallization to a temporal halt by promoting the remobilization of magma batches stored at various levels. In other words, a volcano flank collapse is likely to set off intense magma mixing at depth, an important and long-recognized eruption triggering mechanism (Anderson, 1976), and result in the aggregation of disparate crystal populations, as well as increased eruption rates (e.g., Nakagawa et al., 2002; Ginibre and Wörner, 2007).

In summary, field and petrological evidence as well as the realistic numerical models presented here strongly suggest a cause-and-effect relationship between a large-scale flank collapse—the El Golfo landslide—and the increased eruptive proportions of dense, crystal-rich and mafic magmas at El Hierro Island. Landslide-induced disturbances in the state of stress of a volcano's magmatic system retain relatively large magnitudes down to important depths (e.g., upper mantle at El Hierro) and are likely to drastically alter storage, transport, mixing, differentiation, and degassing of magma batches. These results provide a basis for as-yet unexplained changes in the eruptive and geochemical regimes at volcanoes that have experienced large-scale destructive events.

ACKNOWLEDGMENTS

The German Deutsche Forschungsgemeinschaft (DFG) (grant WA1642/1-4), the Natural Sciences and Engineering Research Council of Canada (NSERC), Trinity College Dublin, and the Science Foundation of Ireland provided project funding. The authors acknowledge discussion with V. Pinel, as well as insightful reviews by J.C. Carracedo, J. Martí, and an anonymous referee. Manconi and Longpré contributed equally to this work.

REFERENCES CITED

Anderson, A.T., 1976, Magma mixing: Petrological process and volcanological tool: Journal of Volcanology and Geothermal Research, v. 1, p. 3–33, doi: 10.1016/0377-0273(76)90016-0.

Andrew, R.E., and Gudmundsson, A., 2007, Distribution, structure, and formation of Holocene lava shields in Iceland: Journal of Volcanology and Geothermal Research, v. 168, p. 137–154, doi: 10.1016/j.jvolgeores.2007.08.011.

Carracedo, J.C., Badiola, E.R., Guillou, H., de la Nuez, J., and Perex Torrado, F.J., 2001, Geology and volcanology of La Palma and El Hierro, western Canaries: Estudios Geológicos, v. 57, p. 175–273.

Ginibre, C., and Wörner, G., 2007, Variable parent magmas and recharge regimes of the Parinacota magma system (N. Chile) revealed by Fe, Mg and Sr zoning in plagioclase: Lithos, v. 98, p. 118–140, doi: 10.1016/j.lithos.2007.03.004.

Hansteen, T.H., Klügel, A., and Schmincke, H.U., 1998, Multi-stage magma ascent beneath the Canary Islands: Evidence from fluid inclusions: Contributions to Mineralogy and Petrology, v. 132, p. 48–64, doi: 10.1007/s004100050404.

Hildenbrand, A., Gillot, P., and Le Roy, I., 2004, Volcano-tectonic and geochemical evolution of an oceanic intra-plate volcano: Tahiti-Nui (French Polynesia): Earth and Planetary Science Letters, v. 217, p. 349–365, doi: 10.1016/S0012-821X(03)00599-5.

Hora, J.M., Singer, B.S., and Wörner, G., 2007, Volcano evolution and eruptive flux on the thick crust of the Andean Central volcanic zone: $^{40}Ar/^{39}Ar$ constraints from Volcán Parinacota, Chile: Geological Society of America Bulletin, v. 119, p. 343–362.

Izbekov, P., Eichelberger, J., Belousova, M., Ozerov, A., and PIRE team, 2006, Post-collapse trends at Bezymianny volcano, Kamchatka, Russia and the May 6, 2006 eruption: Eos (Transactions, American Geophysical Union), v. 87, no. 52.

Jull, M., and McKenzie, D., 1996, The effect of deglaciation on mantle melting beneath Iceland: Journal of Geophysical Research, v. 101, p. 21,815–21,828, doi: 10.1029/96JB01308.

Klügel, A., Hansteen, T.H., and Galipp, K., 2005, Magma storage and underplating beneath Cumbre Vieja volcano, La Palma (Canary Islands): Earth and Planetary Science Letters, v. 236, p. 211–226.

Lipman, P.W., Rhodes, J.M., and Dalrymple, G.B., 1991, The Ninole Basalt—Implications for the structural evolution of Mauna Loa volcano, Hawaii: Bulletin of Volcanology, v. 53, p. 1–19, doi: 10.1007/BF00680316.

Manga, M., and Brodsky, E., 2006, Seismic triggering of eruptions in the far field: Volcanoes and geysers: Annual Review of Earth and Planetary Sciences, v. 34, p. 263, doi: 10.1146/annurev.earth.34.031405.125125.

Masson, D.G., Watts, A.B., Gee, M.J.R., Urgeles, R., Mitchell, N.C., Le Bas, T.P., and Canals, M., 2002, Slope failures on the flanks of the western Canary Islands: Earth-Science Reviews, v. 57, p. 1–35, doi: 10.1016/S0012-8252(01)00069-1.

McGuire, W., 1996, Volcano instability: A review of contemporary themes: Geological Society of London Special Publication 110, p. 1–23.

Nakagawa, M., Wada, K., and Wood, C.P., 2002, Mixed magmas, mush chambers and eruption triggers: Evidence from zoned clinopyroxene phenocrysts in andesitic scoria from the 1995 eruptions of Ruapehu volcano, New Zealand: Journal of Petrology, v. 43, p. 2279–2303, doi: 10.1093/petrology/43.12.2279.

Pinel, V., and Jaupart, C., 2000, The effect of edifice load on magma ascent beneath a volcano: Royal Society Philosophical Transactions–Mathematical, Physical and Engineering Sciences, v. 358, p. 1515–1532.

Pinel, V., and Jaupart, C., 2005, Some consequences of volcanic edifice destruction for eruption conditions: Journal of Volcanology and Geothermal Research, v. 145, p. 68–80, doi: 10.1016/j.jvolgeores.2005.01.012.

Presley, T.K., Sinton, J.M., and Pringle, M., 1997, Postshield volcanism and catastrophic mass-wasting of the Waianae volcano, Oahu, Hawaii: Bulletin of Volcanology, v. 58, p. 597–616, doi: 10.1007/s004450050165.

Sigvaldason, G.E., Annertz, K., and Nilsson, M., 1992, Effect of glacier loading/deloading on volcanism: Postglacial volcanic production rate of the Dyngjufjöll area, central Iceland: Bulletin of Volcanology, v. 54, p. 385–392, doi: 10.1007/BF00312320.

Stroncik, N.A., Klügel, A., and Hansteen, T.H., 2009, The magmatic plumbing system beneath El Hierro (Canary Islands): Constraints from phenocrysts and naturally quenched basaltic glasses in submarine rocks: Contributions to Mineralogy and Petrology, v. 157, p. 593–607.

Walter, T.R., and Amelung, F., 2007, Volcanic eruptions following M >= 9 megathrust earthquakes: Implications for the Sumatra-Andaman volcanoes: Geology, v. 35, p. 539–542, doi: 10.1130/G23429A.1.

Manuscript received 3 February 2009
Revised manuscript received 17 Jul 2009
Manuscript accepted 21 July 2009

Printed in USA